Carbohydrate Polymers 163 (2017) 270–279

Contents lists available at ScienceDirect

Carbohydrate Polymers

journal homepage: www.elsevier.com/locate/carbpol

Inhibition of acrolein-induced autophagy and apoptosis by a glycosaminoglycan from *Sepia esculenta* ink in mouse Leydig cells

Yi-Peng Gu[a,b,1], Xiao-Mei Yang[a,1], Ping Luo[b], Yan-Qun Li[c], Ye-Xing Tao[d], Zhen-Hua Duan[a], Wei Xiao[b], Da-Yan Zhang[d], Hua-Zhong Liu[b,*]

[a] *Institute of Food Science and Engineering Technology, Hezhou University, Hezhou 542899, China*
[b] *College of Chemistry & Environment, Guangdong Ocean University, Zhanjiang 524088, China*
[c] *College of Food Science & Technology, Guangdong Ocean University, Zhanjiang 524088, China*
[d] *Science Experiment Center, Guilin Medical University, Guilin 541004, China*

ARTICLE INFO

Article history:
Received 1 December 2016
Received in revised form 16 January 2017
Accepted 21 January 2017
Available online 23 January 2017

Chemical compounds studied in this article:
Acrolein (PubChem CID: 7847)
Cyclophosphamide (PubChem CID: 2907)
Malondialdehyde (PubChem CID: 10964)
Testosterone (PubChem CID: 6013)
Monodansylcadaverin (PubChem CID: 4247)
Propidium iodide (PubChem CID: 104981)
Osmium tetroxide (PubChem CID: 30318)

Keywords:
Glycosaminoglycan
Sepia esculenta ink
Autophagy
Apoptosis
Leydig cells
Acrolein

ABSTRACT

In our recent reports, a squid ink polysaccharide (SIP) was found having preventive activity against cyclophosphamide induced damage in mouse testis and ovary. Here we further reveal the regulative mechanism of SIP against chemical toxicity on testis. Leydig cells exposed to acrolein (ACR) underwent apoptosis at 12 h and 24 h. Before apoptosis, cells occurred autophagy that was confirmed by high autophagic rate and Beclin-1 protein content at 3 h. PI3K/Akt and p38 MAPK signal pathways involved in the regulatory mechanisms. These outcomes of ACR were recovered completely by SIP, which was demonstrated by attenuated disruption of redox equilibrium and increased testosterone production, through suppressing ACR-caused autophagy and apoptosis regulated by PI3K/Akt and p38 MAPK signal pathways in Leydig cells. Summarily, autophagy occurred before apoptosis caused by ACR-activated p38 MAPK and PI3K/Akt pathways were blocked by SIP, resulting in survival and functional maintenance of Leydig cells.

1. Introduction

As one of the most commonly used chemotherapeutic agents, cyclophosphamide (CP) is widely used for clinical management on several cancers (Emadi, Jones, & Brodsky, 2009). However, a series of undesirably systematic side effects on normal tissues/organs (Emadi et al., 2009) result in reduction of dosage for escaping systematic toxicity and in consequent decrease of therapeutic effects. In order to attenuate the systematic side effects and elevate the efficacy of chemotherapy, complementary and alternative medicine, particularly natural products, has been studied for decades.

A squid ink polysaccharide (SIP), a kind of glycosaminoglycan, has been isolated recently from *Sepia esculenta* ink and verified to be effective in preventing testis and ovary of mice from CP-mediated toxicity in our laboratory (Le, Luo, Gu, Tao, & Liu, 2015a; Le, Luo, Gu, Tao, & Liu, 2015b; Liu et al., 2016). SIP protected mouse ovaries exposed to CP through weakening autophagy to inhibit the apoptosis of ovarian cells, such as granulosa cells, or supressing autophagy-associated cell death to reduce programmed cell death (Liu et al., 2016). The work also revealed that the preventive mechanisms of SIP on mouse ovary were correlated with p38 mitogen-activated protein kinase and Akt-associated signaling pathways (Liu et al., 2016). Interestingly, our another simultaneous investigation found that testicular oxidative stress damage

* Corresponding author at: Guangdong Ocean University, College of Chemistry & Environment, No. 1 Haida Road, Zhanjiang 524088, Guangdong, China.
E-mail address: liuhzbs@163.com (H.-Z. Liu).
[1] The authors equally contribute to this paper.

http://dx.doi.org/10.1016/j.carbpol.2017.01.081
0144-8617/

occurred in the mice exposed to CP and was interfered by SIP via altering protein contents of keap-1 and histone deacetylase 2 to trigger Nrf2/ARE signaling pathway to up-regulate expression of the downstream phase II enzymes and antioxidative enzymes (Le et al., 2015a, 2015b).

It is well known that CP must be metabolized to acrolein (ACR) and phosphoramide mustard by liver-originated enzymes before exerting killing effects on tumor or normal cells (Emadi et al., 2009). So further investigation of the accurate molecular mechanisms for CP to injure cells should be based on *in vitro* experiments of cells treated with ACR or phosphoramide mustard. In order to approach the mechanisms, ACR was used in this study. Key reason of employing ACR is that ACR is a biotransformation product of CP and is also the product of endogenous lipid peroxidation reactions, consumption of cigarettes and intake of automobile exhausts, overheated cooking oils and residual herbicides, which are everywhere in our surroundings and has been proved fully to have toxicity on reproductive system (Kern & Kehrer, 2002; Lewars & Liebman, 2013; Tully, Zheng, Acosta, Tian, & Shi, 2014). Another critical cause is different functions of the two metabolites, i.e., phosphoramide mustard functions in anticancer and ACR is mainly responsible for toxic side effects on normal cells of tissues/organs (Emadi et al., 2009). Therefore, this study aimed to investigate the protective effects of SIP against ACR toxicity on survival and function of mouse Leydig cells, as well as the possible mechanisms.

2. Materials and methods

2.1. Preparation of SIP

According to our methods (Liu et al., 2016), the procedure is modified slightly and briefly discribed as follows. Fresh ink derived from squid sacs (*Sepia esculenta*) was stored at −70 °C and was thawed at 4 °C followed by dilution with PBS and then ultrasonicated. The suspension was stored at 4 °C for more than 8 h and then subjected to centrifugation at 4 °C, 8000 rpm. The supernatant was hydrolyzed with papain for 90 min and then heated to denature the enzyme. The deproteinized ink solution was mixed with four volumes of ethanol. Crude polysaccharides were obtained through recovery of the precipitate and then further separated into three fractions by DEAE-52 cellulose column chromatography. SIP was in the first fraction, that fraction was collected and then dialyzed, concentrated under vacuum, freeze-dried, and stored at −20 °C.

2.2. Cell culture

Primary Leydig cells of mice (purchased from ATCC) were cultured in DMEM/F12 medium supplemented with 10% fetal bovine serum at 37 °C in a 5% CO_2 humidified incubator.

2.3. Cell viability and biochemistry detection

Cell viability was detected with WST-1 assay kit. Testosterone (T) content in medium was measured with enzyme-linked immunosorbent assay kit. Intracellular activity of superoxide dismutase (SOD), total antioxidative ability (TAOC) and content of malondialdehyde (MDA) were determined with kits respectively. The kits were purchased from a bioengineering institute in China.

2.4. Ultrastructure observation

Cells were fixed with 5% glutaraldehyde at 4 °C for 2 h, and then washed three times with PBS followed by post-fixing with 1% osmium tetroxide for 2 h at 4 °C. After washing twice with PBS, cells were dehydrated with ethanol and acetone, embedded in Epon812 and sectioned with an ultra-microtome. The stained sections were observed using transmission electron microscope.

2.5. Double staining of Leydig cells with Annexin V-FITC/PI

Leydig cells were washed twice to remove medium, and added to 500 μl of Binging buffer with 5 μl of Annexin V-FITC and 5 μl of PI. Cells were incubated for 10 min in dark at room temperature. The confocal laser scanning microscope was used to observe apoptosis of Leydig cells.

2.6. Monodansylcadaverin staining of Leydig cells

Leydig cells were washed twice and added monodansylcadaverin (MDC) staining solution before incubating for 30 min in dark at room temperature. The confocal laser scanning microscope was used to observe autophagy of Leydig cells. Image Pro Plus 6.0 software was utilized to analyze MDC-positive cells.

2.7. Flow cytometry assay

Cells were stained with 50 μM MDC for 30 min at 37 °C, trypsinized, washed, and collected in PBS. Cells illuminated with

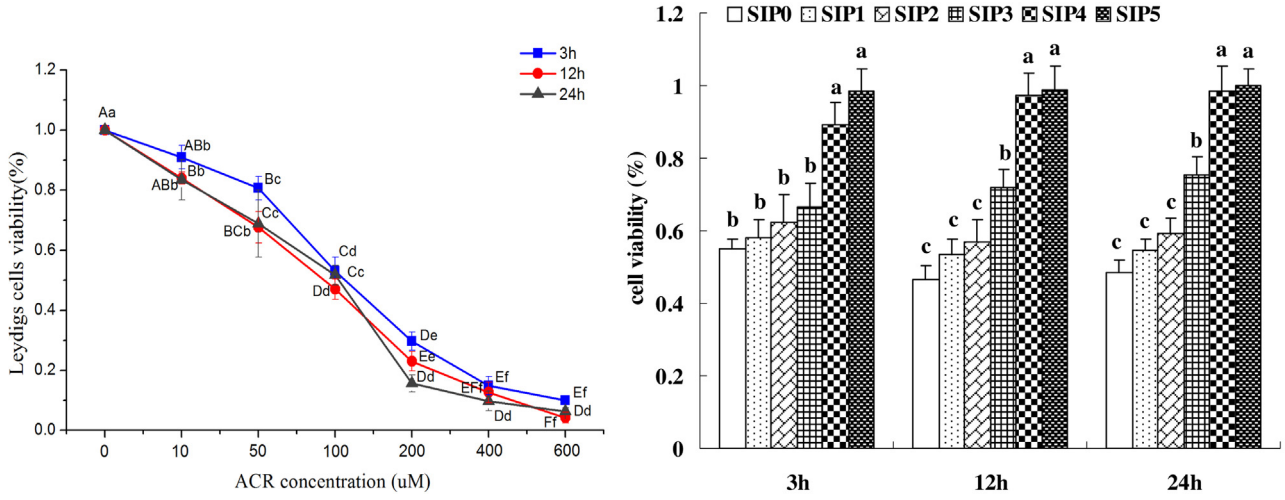

Fig. 1. SIP inhibited ACR mediated death of Leydig cells. Primary Leydig cells of mice grown to 70% confluence were exposed to ACR (0, 10, 50, 100, 200, 400 and 600 μmol/L) and different concentrations of SIP (0, 0.1, 0.2, 0.5, 1 and 2 mg/ml, corresponding to SIP0, SIP1, SIP2, SIP3, SIP4 and SIP5 respectively) for 3, 12 and 24 h respectively. Cell viability was measured with WST-1 assay. $^{abcdef}p < 0.05$.

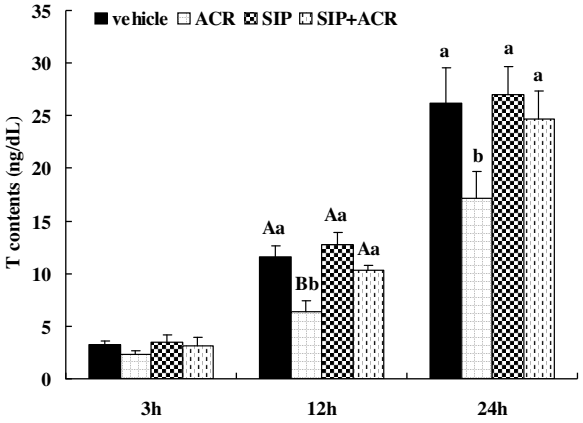

Fig. 2. SIP recovered testosterone production of Leydig cells destroyed by ACR. Leydig cells were cultured for 3, 12 and 24 h under treatment of ACR (140 μmol/L) and SIP (1 mg/ml) respectively. Medium was harvested to measure testosterone content with enzyme-linked immunosorbent assay kit developed by a biological engineering institute of China. $^{ab}p < 0.05$, $^{AB}p < 0.01$.

blue excitation light was measured with flow cytometer. Depending on their acidity, autophagic lysosomes appeared as the fluorescent cytoplasmic vesicles, autophagy was quantified as a fluorescence intensity.

2.8. Western blotting assay

Cells were lysed in ice-cold non-denaturing cell lysis buffer. Protein lysate was denatured in protein sample buffer with boiling water, and subjected to SDS polyacrylamide gel electrophoresis. Protein was transferred to nitrocellulose membranes and probed with specific antibody. The membranes were visualized with SuperSignal West Pico chemi-luminescence detection system.

2.9. Statistical analysis

Data were presented as mean ± standard deviation and analyzed using SPSS 19.0 software. One-way analysis of variance (ANOVA) and the post hoc Tukey HSD test were used to evaluate differences between groups. $p < 0.05$ and $p < 0.01$ were considered significant.

3. Results

3.1. SIP elevates viability of Leydig cells exposed to ACR in a dose-dependent manner

According to the curve of Leydig cells viability determined by WST-1 analysis (Fig. 1), ACR suppressed proliferation of Leydig cells and the inhibitory effect behaved dose-dependent. The cell viability correlated negatively with ACR concentration ($r_{3h} = -0.901$, $r_{12h} = -0.887$, $r_{24h} = -0.864$; $p < 0.01$). At the time-points of 3, 12

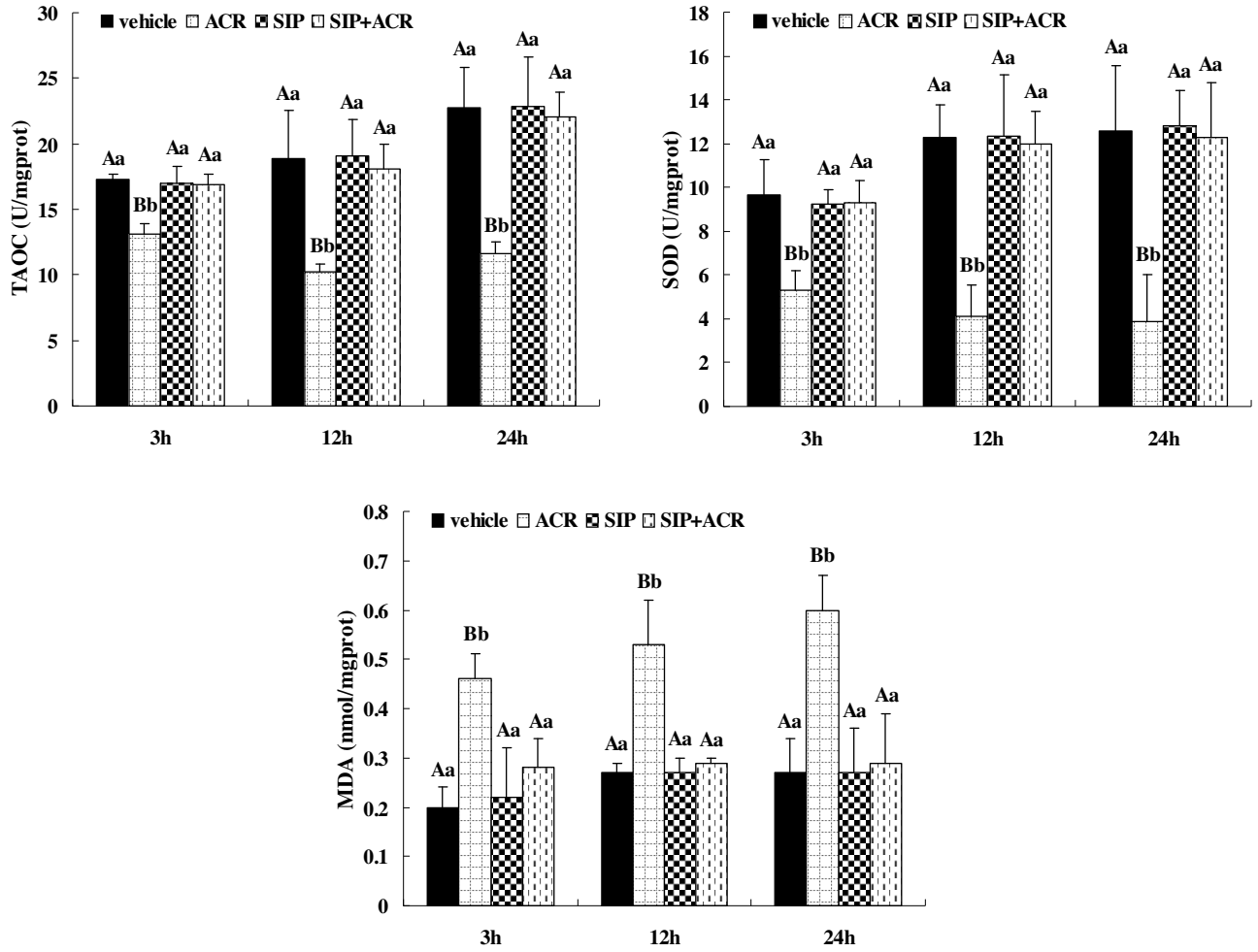

Fig. 3. ACR altered antioxidative ability of Leydig cells was reversed by SIP. Leydig cells were treated with ACR and/or SIP for the scheduled time and were then washed with PBS. Cells were lysed in nondenature lysis buffer. Activity of superoxide dismutase, total antioxidant capacity and malondialdehyde content were detected with kits respectively according to manufacturer's procedure. $^{ab}p < 0.05$, $^{AB}p < 0.01$.

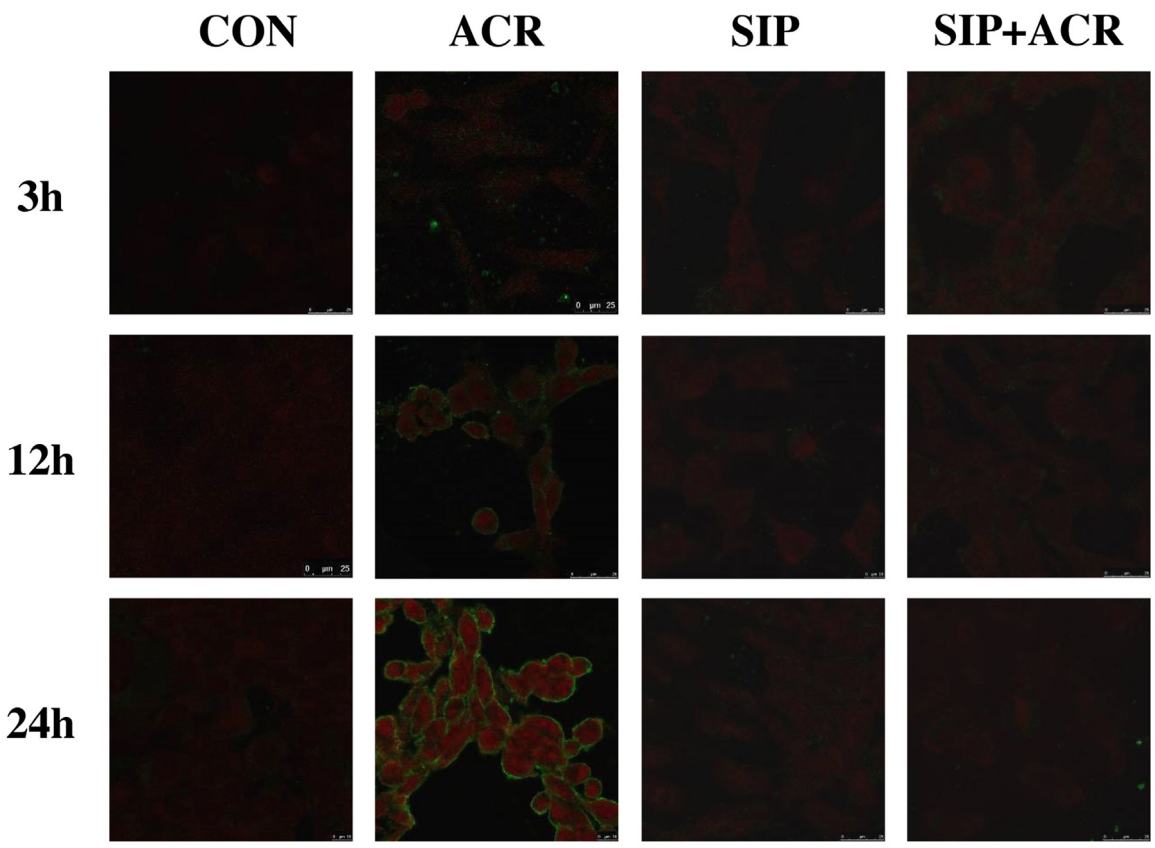

Fig. 4. Apoptosis in ACR treated Leydig cells was relieved by SIP. Leydig cells were treated with ACR and/or SIP for 3, 12 and 24 h respectively and were subjected to detection of apoptosis using confocal laser scanning microscopy.

and 24 h, ACR IC_{50} was 191.08, 144.43 or 140.35 μmol/L respectively. A concentration of 140.0 μmol/L was chosen as the optimal dose of ACR in following experiments.

The toxicity of ACR on Leydig cells was obviously presented under the vehicle and low SIP dosage (0.1 and 0.2 mg/ml) treatment. Particularly vehicle treated cells without SIP protection showed a lower viability. Although low dosage of SIP effectively blocked the decrease of cell viability, a failure in promoting cell viability was also appeared. However, it was clearly observed that high dosage of SIP successfully reversed the negative effects of ACR, improving the viability of Leydig cells, and that gradually incremental SIP generated higher viability, especially at the dosage of 1.0 and 2.0 mg/ml SIP. From Fig. 1, it can be found that a dose-dependent positive relationship occurred between SIP concentration and viability of Leydig cells exposed to ACR. Since significant difference was not observed between 1.0 and 2.0 mg/ml SIP administered groups, both were markedly better than 0.5 mg/ml SIP group at the three scheduled time-points (3 h, 12 h and 24 h), 1.0 mg/ml was chosed to be the optimal dose in this study.

3.2. SIP promotes testosterone production and antioxidative ability of Leydigcells

Data presented in Fig. 2 indicated a pronounced decrease of testosterone (T) content in ACR stimulated Leydig cells, except for 3 h. Although SIP failed to alter T contents in the medium of vehicle treated cells, a remarkable elevation of T production was found in the Leydig cells co-treated with SIP and ACR. The data also suggested that ACR disrupted secretory function of Leydig cells was rescued by SIP, which implied that ACR was able to destroy the male reproductive cells when SIP was absent.

Similar results were also observed in antioxidative ability of Leydig cells (Fig. 3). ACR not only reduced total antioxidative capacity and superoxide dismutase activity in Leydig cells, also promoted lipid oxidation (increase of malonaldehyde content) and consequent disruption of membrane. Fortunately, the presence of SIP enabled the recovery of the ACR injured cells to normal.

From the above results, it can be deduced that ACR initiated oxidative stress in Leydig cells to damage antioxidant system and resultant cellular secretory function, but the cellular toxicity of ACR was effectively relieved by SIP.

3.3. SIP suppresses induction of apoptosis

In order to approach the inhibitory mechanism of SIP against ACR-mediated disruption of Leydig cells, apoptosis was investigated using annexin V/PI double-staining, confocal laser scanning microscope and western blot assay. Comparing with the vehicle treated cells, the ACR treated cells appeared apoptosis at 12 h, and 24 h but no obvious apoptosis-associated morphological features at 3 h. Under administration of SIP, morphological features of apoptosis in ACR co-treated cells disappeared, nearly no difference was observed between the co-stimulated and vehicle treated cells (Fig. 4).

In consistent with morphological alternation of apoptosis, apoptosis-associated proteins expression profiles were also modified under management of ACR and/or SIP (Fig. 5). ACR significantly reduced antiapoptotic gene bcl-2 translation from 3 h to the end, and markedly promoted expression of two proapoptotic genes, bax and caspase-3, after 12 h, which indicated occurrence of apoptosis induced by ACR. SIP successfully inhibited the ACR mediated programmed cell death, demonstrated by increase of content of

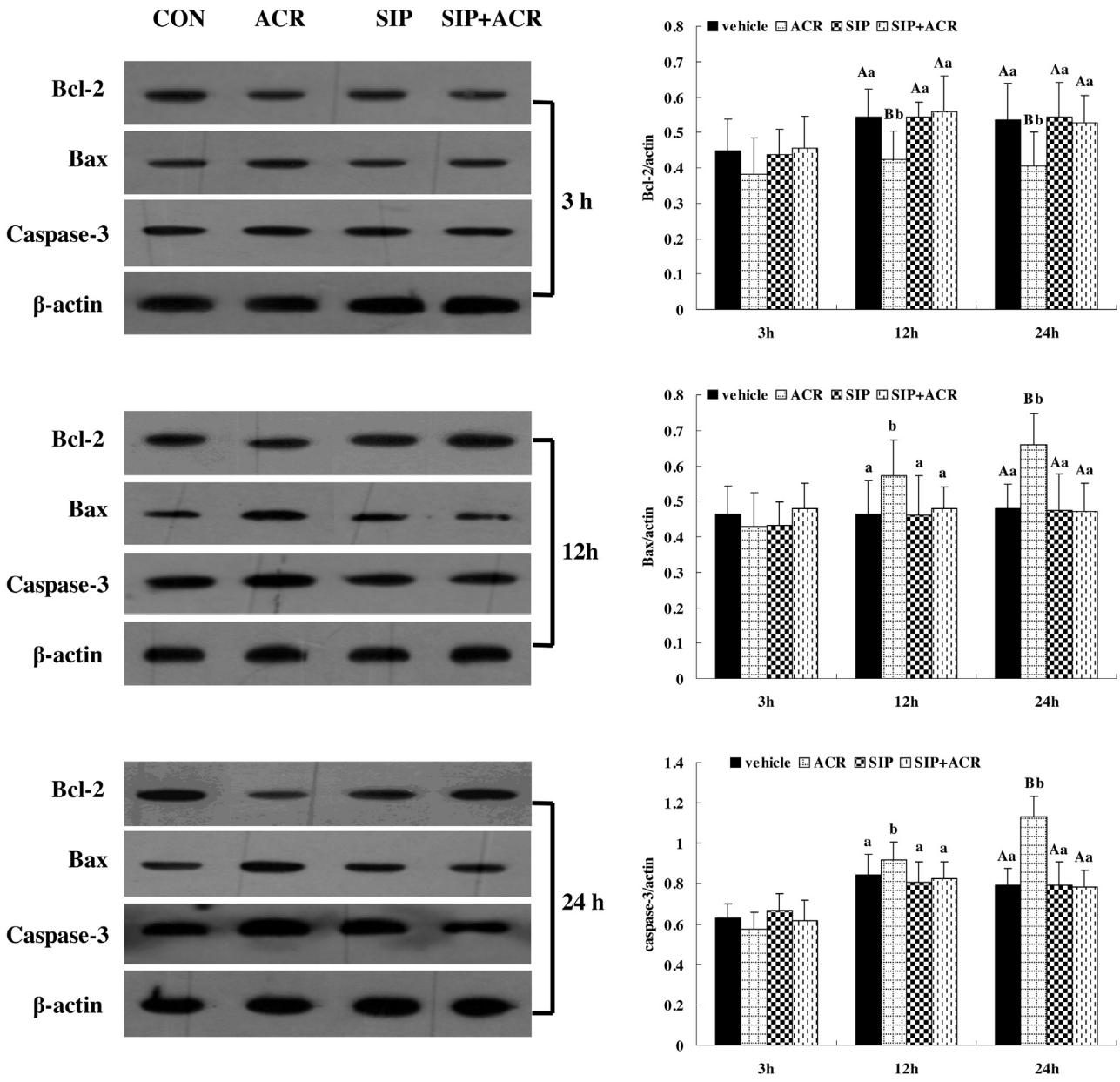

Fig. 5. SIP modified the expression profile of apoptosis related proteins ACR induced in Leydig cells. Leydig cells were treated with ACR and/or SIP for 3, 12 and 24 h respectively and were subjected to detection of apoptosis using western blotting. Different letters indicate significant differences, $^{ab}p < 0.05$, $^{AB}p < 0.01$.

Bcl-2 protein and reduction of Bax and Caspase-3 proteins, nearly equivalent to vehicle or SIP treated cells.

Above-mentioned data definitely present that ACR enables Leydig cells to occur apoptosis, which is suppressed by SIP, suggesting that SIP can prevent Leydig cells from ACR initiated apoptosis. Then which biological mechanism in ACR-treated Leydig cells has been employed by SIP for preventing chemical toxicity?

3.4. SIP weakens ACR induced autophagy

It is now well known that autophagy plays important roles in regulating programmed cell death. To learn whether or not autophagy was involved in the actions of ACR and SIP on apoptosis, autophagy was evaluated with monodansylcadaverin staining, confocal laser scanning microscope, flow cytometry and western blot assay. Fig. 6 revealed that autophagy rate in ACR administered cells was much higher than that in vehicle and SIP treated cells after treatment for 3 h. Although SIP could not decline the amazing autophagy rate ACR caused to the normal levels as in vehicle or SIP treated cells, the autophagy rate in the cells co-stimulated with SIP and ACR was found a dramatical decrease compared with ACR treated cells. However, after treatments for 12 h and 24 h, every group of cells showed almost identical low autophagy rate, no significant difference was observed among them.

The expression level of Beclin-1 protein, an important marker protein of autophagy, was consistent with the changes in morphology and quantity in Leydig cells. At 3 h, Beclin-1 content in ACR injured cells was significant higher than that in vehicle treated cells, but the exposure to SIP affected the protein expression. Similarly, at 12 h and 24 h, significant differences of the protein contents were not observed among four groups of cells (Fig. 7).

Considering the autophagy and apoptosis occurred in ACR and/or SIP treated Leydig cells, it could be deduced that both ACR-induced autophagy of early phase (3 h) and apoptosis of mid-late phase (12 and 24 h) were suppressed by SIP. Intracellular autophagy- and apoptosis-associated signaling pathways have

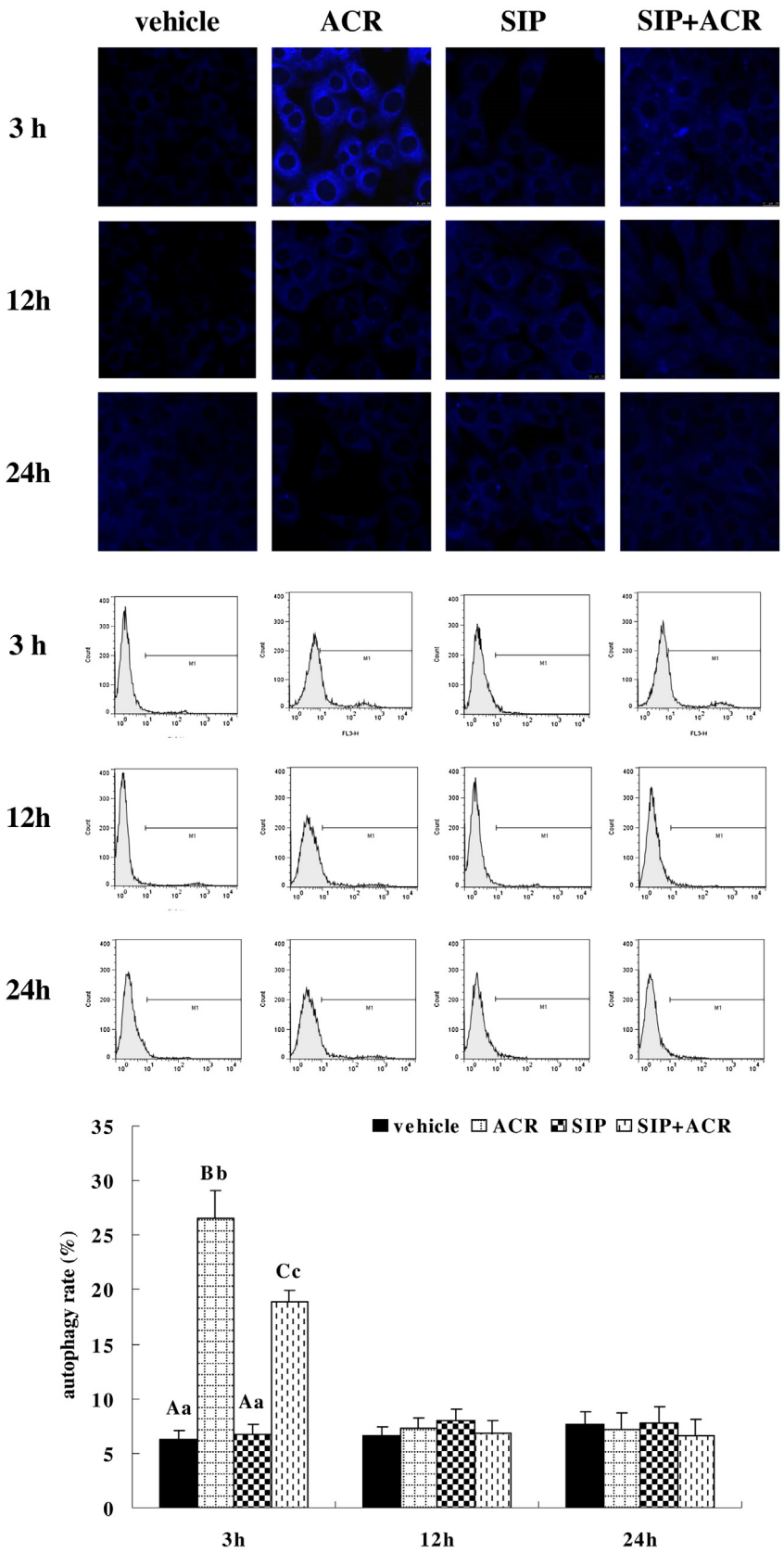

Fig. 6. ACR-induced autophagy of Leydig cells was inhibited by SIP. Leydig cells were treated with ACR and/or SIP for 3 h, 12 h and 24 h respectively and were subjected to detect autophagy with monodansylcadaverin staining, confocal laser scanning microscope and flow cytometry methods. Different letters indicate significant differences, $^{abc}p < 0.05$, $^{AB}p < 0.01$.

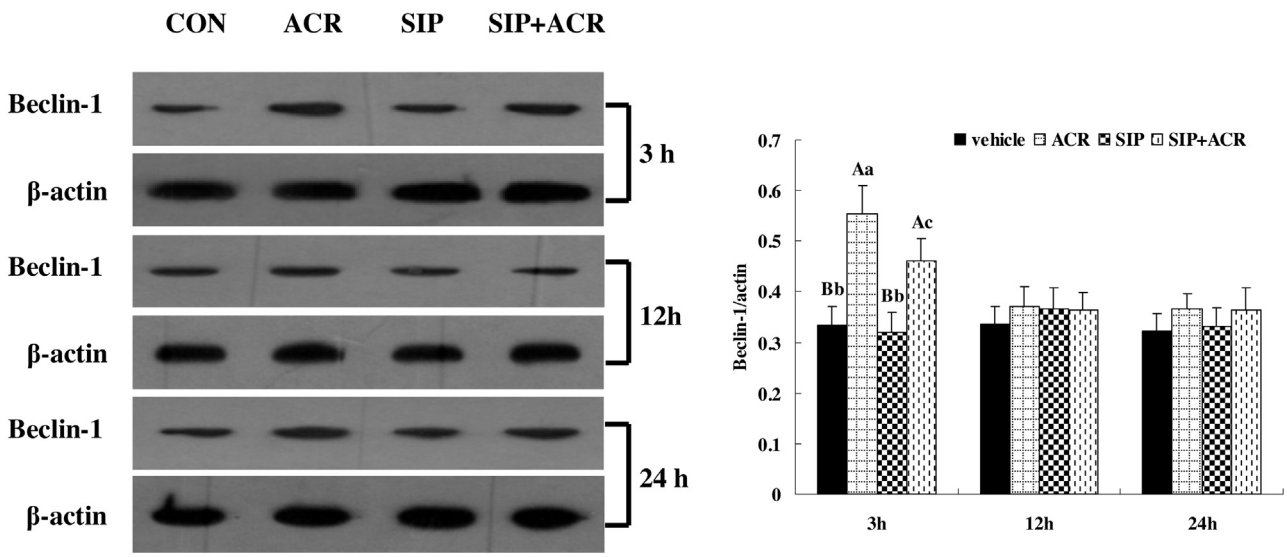

Fig. 7. Alteration of autophagy-associated protein Beclin-1 in ACR exposed Leydig cells was suppressed by SIP. Leydig cells were treated with ACR and/or SIP for 3 h, 12 h and 24 h respectively and were subjected to detect contents of autophagy-associated protein, Beclin-1, with western blotting method. Different letters indicate significant differences, $^{abc}p < 0.05$, $^{AB}p < 0.01$.

been verified to be various and complicated. Which pathways participate in the intervention mechanisms of SIP against ACR-induced autophagy and apoptosis of Leydig cells would be further studied in this article.

3.5. SIP employs p38 MAPK and PI3K/Akt signaling pathways to impair ACR induced autophagy and apoptosis in Leydig cells

Fig. 8 showed that throughout the experiment phosphorylation levels of both p38 and Akt proteins in ACR treated cells were significantly higher than in vehicle stimulated cells, and SIP exposure clearly declined the contents of phospho-p38 and −Akt proteins. The results demonstrated that p38- and Akt-associated signaling pathways were activated by ACR and suppressed by SIP. It was also found that in the cells co-treated with SIP and ACR, contents of both phospho-p38 and −Akt proteins were nearly identical to that in vehicle or SIP administered cells, no obvious difference was found among the three groups of cells.

Now we can conclude that SIP inhibits ACR-caused autophagy and apoptosis in Leydig cells via inactivating ACR-triggered p38 MAPK and PI3K/Akt signaling pathways.

4. Discussion

Our recent findings (Liu et al., 2016) discovered a glycosaminoglycan from Sep*ia esculenta* ink, which is dominantly composed of arabinose and galactosamine and differs from the published cuttlefish ink polysaccharides (Chen et al., 2008; Liu et al., 2008; Takaya, Uchisawa, Narumi, & Matsue, 1996).

It has been verified in our previous studies that CP caused oxidative stress in mouse testes can be weakened by SIP through activation of Nrf2/ARE signaling pathway (Le et al., 2015a, 2015b). As a commonly used chemotherapeutic agent, CP must be metabolized to two active derivatives, phosphoramide mustard and ACR, by liver-originated enzymes (Emadi et al., 2009). Phosphoramide mustard is associated with CP's antineoplastic effects, and ACR is linked with the toxic side effects, such as reproductive toxicity (Emadi et al., 2009). Aside from as a metabolite of CP, ACR may also come from cigarette, endogenous lipid peroxidation reactions, automobile exhausts, overheated cooking oils and herbicides, etc. (Kern & Kehrer, 2002; Lewars & Liebman, 2013; Tully et al., 2014). Therefore, the toxicity on testicular germ cells shoud be urgently approached to escape from ACR exposure. Leydig cell employed in this research is the main secretor of testosterone, which is an indispensable steroid hormone for both spermatogenesis and sex characteristic of male (Handelsman, 2011).

ACR not only damages proteins, DNA and lipids in various cell types (Tully et al., 2014), but also destroys antioxidative ability, resulting in disruption of redox equilibrium (Kehrer & Biswal, 2000; Roy, Pallepati, Bettaieb, Tanel, & Averill-Bates, 2009). Our current study showed decrease of testosterone production and lose of antioxidant capacity demonstrated by reduction of intracellular TAOC and SOD activity and increment of lipid peroxidation in ACR treated Leydig cells, and the results confirmed that ACR induced oxidative stress destroyed the male germ cells. Meanwhile, morphology characteristic of apoptosis emerged in the damaged cells at the middle and later stage of treatment (12 h and 24 h) with annexin V-FITC/PI staining, which was demonstrated by alternation of three key proteins contents, drop of anti-apoptotic protein Bcl-2 and augment of pro-apoptotic proteins Caspase-3 and Bax. The results were very similar to a reported investigation about another kind of male germ cell, Sertoli cell (Liu et al., 2012). Liu et al. (2012) revealed that apoptosis occurred when Sertoli cells exposed to ACR for 12 h. Although in the early stage of treatment (3 h) apoptosis was not an outcome of ACR induction to Leydig cells, autophagy occurred pronouncedly and disappeared in the process of apoptosis. Apart from skyscraping autophagy rate caused by ACR, Beclin-1 translation was also upregulated. Beclin-1, a mammalian homolog of yeast Vps30/Atg6, binds PI3K III to forms a complex that involves in the formation of autophagosomes and initiation of macroautophagy, generally called autophagy (Klionsky et al., 2016). Bcl-2 inhibits autophagy via interaction with Beclin-1 avoiding formation of Beclin-1/PI3K-III and via inhibiting Bax and Bak-1 (Klionsky et al., 2016). In the middle and later phase of ACR treatment, reduction of Bcl-2 and increase of Bax implied that Bcl-2 was unable to inhibit autophagy, moreover autophagy was now undetectable. Incremental Beclin-1 at 3 h expressed an occurring autophagy, and the normal content of Beclin-1 at 12 h and 24 h displayed absence of autophagy.

However, it is worth noting that the activated Akt protein expression under ACR exposure means participation of PI3K/Akt/mTOR pathway in the regulatory process. Generally

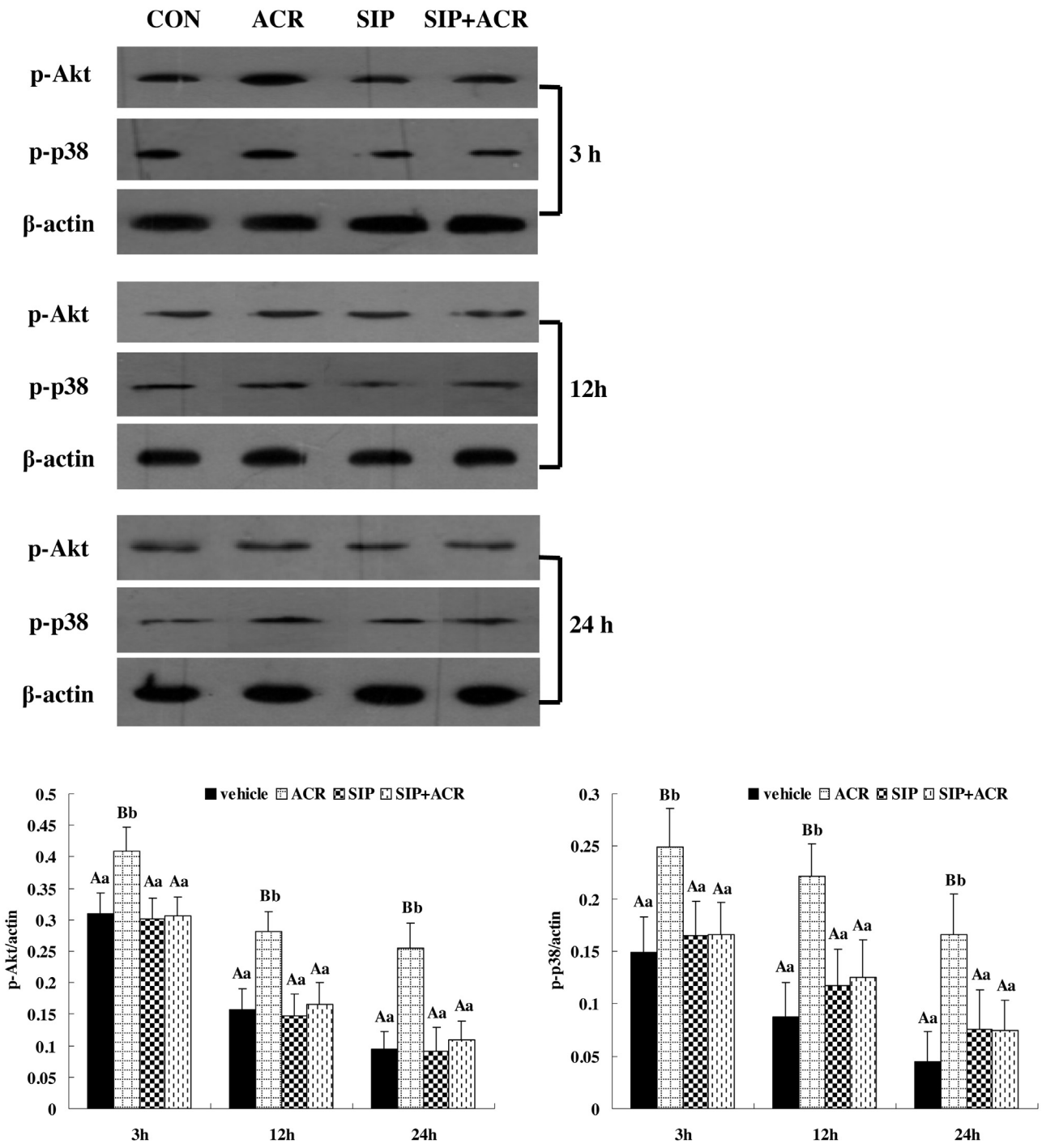

Fig. 8. Increase of Akt and p38 proteins phosphorylation ACR caused was reduced by SIP in Leydig cells. Leydig cells were treated with ACR and/or SIP for 3 h, 12 h and 24 h respectively and were subjected to detect phosphorylation of Akt and p38 proteins with western blotting method. Different letters indicate significant differences, $^{ab}p < 0.05$, $^{AB}p < 0.01$.

PI3K/Akt/mTOR pathway is believed to negatively regulate autophagy in some cellular systems (Klionsky et al., 2016). In addition, PI3K/Akt is a cell survival pathway, and the phosphorylated Akt promotes the cell survival by phosphorylating and inactivating the pro-apoptotic factors, as a result inhibiting apoptosis occurrence (Johnson-Holiday et al., 2011; Radin, Lippa, Patel, & Leonardi, 2016). Some researches have reported the induction of autophagy via PI3K/Akt/mTOR pathway activation (Du et al., 2014; Rautou et al., 2010; Sun, Wang, & Yakisich, 2013; Wang, Guo, Wang, & Qian, 2013; Wu, 2014). Therefore, we can suppose reasonably that ACR activated PI3K/Akt pathway to induce autophagy of Leydig cells at 3 h and to inhibit autophagy and promote apoptosis at 12 h and 24 h. Besides, the p38 MAPK signal pathway is also confirmed to negatively regulate autophagy and to induce apoptosis and autophagy-associated cell death (Klionsky et al., 2016; Lemasters et al., 1998; Olson & Hallahan, 2004; Nagelkerke, Sweep, Geurte-Moespot, Bussink, & Span, 2015). p38 MAPK has a dual role in autophagy, both positive and negative regulator. It is possible that the autophagic response may depend upon the nature of the stimulus and the strength and duration of the activated MAPK path-

way (Matsuzawa et al., 2012; Moruno-Manchon, Perez-Jimenz, & Knecht, 2013; Thyagarajan et al., 2010; Webber, 2010). In this work, activation of p38 protein throughout the experiment in ACR administered Leydig cells can be logically speculated to induce autophagy at 3 h for further promoting ACR induced apoptosis at 12 h and 24 h.

Now it is time to discuss the effects and the action mechanisms of SIP on regulating ACR induced apoptosis and autophagy of Leydig cells. The antioxidative ability, which might be destroyed by ACR resulting in disruption of redox equilibrium in Leydig cells, was high effectively protected by SIP, which was similar with our *in vivo* experiments. Testes of mice exposed to CP were observed pronounced oxidant stress damage that was attenuated by SIP through activating Nrf2/ARE signal pathway (Le et al., 2015a, 2015b). The rescued Leydig cells by SIP produced normal content of testosterone, which was demonstrated in the apoptosis and autophagy detection tests. ACR caused damage of protein, DNA and lipids, and the disruption of redox equilibrium should induce apoptosis and autophagy (Cheng et al., 2013; Kroemer, Marino, & Levine, 2010; Li, Ishdorj, & Gibson, 2012; Lin et al., 2012). Our data revealed that ACR mediated apoptosis and autophagy in Leydig cells at different treatment stage, mainly autophagy in the early phase and apoptosis in middle and later phases. Inhibition of SIP on the induced apoptosis and autophagy was verified to be related to p38 MAPK and PI3K/Akt pathways. In our another *in vivo* work, we found that CP activated p38 MAPK pathway and inactivated PI3K/Akt pathway in ovary of mouse, and that SIP weakened CP toxicity on ovary via p38 MAPK and PI3K/Akt signal transduction pathways to suppress CP mediated apoptosis and autophagy (Liu et al., 2016). In this *in vitro* study, SIP also employed p38 MAPK and PI3K/Akt signal pathways to regulate ACR induced apoptosis and autophagy for preventing cytotoxicity in Leydig cells.

5. Conclusion

In summary, two important viewpoints can be drawn from this work. Firstly, autophagy and apoptosis in Leydig cells can be induced by ACR, and autophagy occurrs before apoptosis. During early phase of treatment, ACR induces oxidative stress and consequent disruption of redox equilibrium that results in failure of secretory function. Meanwhile oxidative stress initiates autophagy in Leydig cells. With the proceeding of treatment time, autophagy activates apoptosis-associated signaling pathways that promote induction of apoptosis of Leydig cells to programmed death. At this time, autophagy declines to the state identical to vehicle-treated cells. The results imply that autophagy initiates and promotes apoptosis, which suggests that ACR induced toxicity on Leydig cells is closely related to two important cellular physiological processes, autophagy and apoptosis. Secondly, SIP can effectively affect ACR-mediated autophagy and apoptosis in Leydig cells. At the early phase, ACR caused autophagy can be suppressed by SIP, whereas apoptosis is undetectable difference. After ACR-mediated autophagy actuates apoptosis, apoptotic characteristics becomes more and more visible in ACR-exposed cells, however, in SIP and ACR co-treated cells a decreased apoptosis level can be seen compared with ACR treated Leydig cells. Moreover occurrence of autophagy and apopyosis in Leydig cells exposed to ACR and/or SIP was closely correlated with p38 MAPK and PI3K/Akt signal transduction cascades.

Acknowledgments

This work was supported by the National Natural Science Foundation of China (Grant No. 31171667) and the Natural Science Foundation of Guangdong Province, China (Grant No. 2016A030313753).

References

Chen, S., Xu, J., Xue, C., Dong, P., Sheng, W., Yu, G., et al. (2008). Sequence determination of a non-sulfated glycosaminoglycan-like polysaccharide from melanin-free ink of the squid *Ommastrephes bartrami* by negative-ion electrospray tandem mass spectrometry and NMR spectroscopy. *Glycoconjugate Journal*, *25*, 481–492.

Cheng, P., Ni, Z., Dai, X., Wang, B., Ding, W., Smith, A. R., et al. (2013). The novel BH-3 mimetic apogossypolone induces Beclin-1- and ROS-mediated autophagy in human hepatocellular carcinoma cells. *Cell Death & Disease*, *4*, e489.

Du, T., Huang, H., Chen, X., Ding, H., Zhang, R., Liu, M. L., et al. (2014). LPS regulates macrophage autophagy through PI3K/Akt/mTOR pathway. *Chinese Journal of Pathophysiology*, *30*, 675–680.

Emadi, A., Jones, R. J., & Brodsky, R. A. (2009). Cyclophosphamide and cancer: Golden anniversary. *Nature Reviews Clinical Oncology*, *6*, 638–647.

Handelsman, D. J. (2011). Hormonal regulation of spermatogenesis: Insights from constructing genetic models. *Reproduction Fertility and Development*, *4*, 507–519.

Johnson-Holiday, C., Singh, R., Johnson, E. L., Grizzle, W. E., Lillard, J. W., Jr., & Singh, S. (2011). CCR9-CCL25 interactions promote cisplatin resistance in breast cancer cell through Akt activation in a PI3K-dependent and FAK-independent fashion. *World Journal of Surgical Oncology*, *9*, 46.

Kehrer, J. P., & Biswal, S. S. (2000). The molecular effects of acrolein. *Toxicological Sciences*, *57*, 6–15.

Kern, J. C., & Kehrer, J. P. (2002). Acrolein-induced cell death: A caspase-influenced decision between apoptosis and oncosis/necrosis. *Chemico-Biological Interactions*, *139*, 79–95.

Klionsky, D. J., Abdelmohsen, K., Abe, A., Abedin, M. J., Abeliovich, H., Arozena, A. A., et al. (2016). Guidelines for the use and interpretation of assays for monitoring autophagy (3rd edition). *Autophagy*, *12*, 1–222.

Kroemer, G., Marino, G., & Levine, B. (2010). Autophagy and the integrated stress response. *Molecular Cell*, *40*, 280–293.

Le, X. Y., Luo, P., Gu, Y. P., Tao, Y. X., & Liu, H. Z. (2015a). Interventional effects of squid ink polysaccharides on cyclophosphamide-associated testicular damage in mice. *Bratislava Medical Journal-Bratislavske Lekarske Listy*, *116*, 334–339.

Le, X. Y., Luo, P., Gu, Y. P., Tao, Y. X., & Liu, H. Z. (2015b). Squid ink polysaccharides reduces cyclophosphamide-induced testicular damage via Nrf2/ARE activation pathway in mice. *Iranian Journal of Basic Medical Sciences*, *18*, 827–831.

Lemasters, J. J., Nieminen, A. L., Qian, T., Trost, L. C., Elmore, S. P., Nishimura, Y., et al. (1998). The mitochondrial permeability transition in cell death: A common mechanism in necrosis, apoptosis and autophagy. *BBA-Bioenergetics*, *1366*, 177–196.

Lewars, E., & Liebman, J. F. (2013). What are the enthalpy of formation and the stabilization energy of acrolein? *Structural Chemistry*, *24*, 741–744.

Li, L., Ishdorj, G., & Gibson, S. B. (2012). Reactive oxygen species regulation of autophagy in cancer: Implications for cancer treatment. *Free Radical Biology and Medicine*, *53*, 1399–1410.

Lin, C. J., Lee, C. C., Shih, Y. L., Lin, T. Y., Wang, S. H., Lin, Y. F., et al. (2012). Resveratrol enhances the therapeutic effect of temozolomide against malignant glioma in vitro and in vivo by inhibiting autophagy. *Free Radical Biology and Medicine*, *52*, 377–391.

Liu, C. H., Li, X. D., Li, Y. H., Feng, Y., Zhou, S., & Wang, F. S. (2008). Structural characterization and antimutagenic activity of a novel polysaccharide isolated from Sepiella maindroni ink. *Food Chemistry*, *110*, 807–813.

Liu, F., Li, X. L., Lin, T., He, D. W., Wei, G. H., Liu, J. H., et al. (2012). The cyclophosphamide metabolite, acrolein, induces cytoskeletal changes and oxidative stress in Sertoli cells. *Molecular Biology Reports*, *39*, 493–500.

Liu, H. Z., Tao, Y. X., Luo, P., Deng, C. M., Gu, Y. P., Yang, L., et al. (2016). Preventive effects of a novel polysaccharide from Sepia esculenta ink on ovarian failure and its action mechanisms in cyclophosphamide-treated mice. *Journal of Agricultural and Food Chemistry*, *64*, 5759–5766.

Matsuzawa, T., Kim, B. H., Shenoy, A. R., Kamitani, S., Miyake, M., & Macmicking, J. D. (2012). IFN-γ elicits macrophage autophagy via the p38 MAPK signaling pathway. *Journal of Immunology*, *189*, 813–818.

Moruno-Manchon, J. F., Perez-Jimenz, E., & Knecht, E. (2013). Glucose induces autophagy under starvation conditions by a p38 MAPK-dependent pathway. *Biochemical Journal*, *449*, 497–506.

Nagelkerke, A., Sweep, F. C. G. J., Geurte-Moespot, A., Bussink, J., & Span, P. N. (2015). Therapeutic targeting of autophagy in cancer. Part I: Molecular pathways controlling autophagy. *Seminars in Cancer Biology*, *31*, 89–98.

Olson, J. M., & Hallahan, A. R. (2004). p38 MAP kinase: A convergence point in cancer therapy. *Trends in Molecular Medicine*, *10*, 125–129.

Radin, D., Lippa, A., Patel, P., & Leonardi, D. (2016). Lifeguard inhibition of Fas-mediated apoptosis mechanism for explaining the cisplatin resistance of triple-negative breast cancer cells. *Biomedicine & Pharmacotherapy*, *77*, 161–166.

Rautou, P. E., Mansouri, A., Lebrec, D., Durand, F., Valla, D., & Moreau, R. (2010). Autophagy in liver diseases. *Journal of Hepatology*, *53*, 1123–1134.

Roy, J., Pallepati, P., Bettaieb, A., Tanel, A., & Averill-Bates, D. A. (2009). Acrolein induces a cellular stress response and triggers mitochondrial apoptosis in A549 cells. *Chemico-Biological Interactions*, *181*, 154–167.

Sun, H., Wang, Z., & Yakisich, J. S. (2013). Natural products targeting autophagy via the PI3K/Akt/mTOR pathway as anticancer agents. *Anti-Cancer Agents in Medicinal Chemistry*, *13*, 1048–1056.

Takaya, Y., Uchisawa, H., Narumi, F., & Matsue, H. (1996). Illexins A, B, and C from squid ink should have a branched structure. *Biochemical and Biophysical Research Communications*, *226*, 335–338.

Thyagarajan, A., Jedinak, A., Nguyen, H., Terry, C., Baldridge, L. A., Jiang, J., et al. (2010). Triterpenes from Ganoderma lucidum induce autophagy in colon cancer through the inhibition of p38 mitogen-activated kinase (p38 MAPK). *Nutrition and Cancer*, *62*, 630–640.

Tully, M., Zheng, L., Acosta, G. H. G., Tian, R., & Shi, R. (2014). Acute systemic accumulation of acrolein in mice by inhalation at a concentration similar to that in cigarette smoke. *Neuroscience Bulletin*, *30*, 1017–1024.

Wang, P., Guo, Q. S., Wang, Z. W., & Qian, H. X. (2013). HBx induces HepG-2 cells autophagy through PI3K/Akt/mTOR pathway. *Molecular and Cellular Biochemistry*, *372*, 161–168.

Webber, J. L. (2010). Regulation of autophagy by p38α MAPK. *Autophagy*, *16*, 292–293.

Wu, X. Q. (2014). *Akt phosphorylation regulates autophagy and the C77 of fungi secondary metabolites affacts autophagy and HBV replication*. pp. 5. Hefei: Thesis of Anhui University.